

Slag Treatment Followed by Acid Leaching as a Route to Solar-Grade Silicon

YULIA V. METELEVA-FISCHER,^{1,4} YONGXIANG YANG,² ROB BOOM,^{1,2}
BERT KRAAIJVELD,³ and HENK KUNTZEL³

1.—Materials innovation institute (M2i), Mekelweg 2, 2628CD Delft, The Netherlands.
2.—Department of Materials Science and Engineering, Delft University of Technology, Mekelweg 2, 2628CD Delft, The Netherlands. 3.—RGS Development B.V., Bijlestaal 54, 1721 PW Broek op Langedijk, The Netherlands. 4.—e-mail: y.meteleva-fischer@m2i.nl; ymfischer@gmail.com

Refining of metallurgical-grade silicon was studied using a process sequence of slag treatment, controlled cooling, and acid leaching. A slag of the Na₂O-CaO-SiO₂ system was used. The microstructure of grain boundaries in the treated silicon showed enhanced segregation of impurities, and the formation of CaSi₂ and other Ca-rich phases. Boron and phosphorus were found in the grain boundary phases of silicon after the slag treatment and were successfully removed together with most of the metallic impurities by acid leaching. The interaction between silicon and slag and the distribution of impurities are discussed. A novel mechanism of the refining approach is proposed, based on the microstructure of silicon and the analysis of impurities at each refining step. Parallel processes of slag refining, segregation, and solvent refining were observed, which explains the relatively high efficiency of the proposed refining technology. The investigated combination of refining processes followed by acid leaching has great potential as an efficient and cost-saving route for upgrading metallurgical-grade to solar-grade silicon.

INTRODUCTION

Refining of metallurgical-grade silicon (MG-Si) is a very important scientific topic in silicon research nowadays due to its potential as a cheaper and efficient alternative route to the Siemens process. Slag refining is one of the promising methods proposed for removal of phosphorus and boron from impure silicon. This method based on the principle of liquid-liquid extraction is successfully applied in the steel industry for removal of sulfur and phosphorus.¹ Various silica-based systems have been investigated for refining of MG-Si, all of which emphasize the role of high oxygen potential in the refining process. Additions of the following oxides to silica showed improvement of removal of boron: CaO,² MgO,²⁻⁶ BaO,³⁻⁶ Na₂O,^{3,4,7,8} Li₂O,⁵ and Al₂O₃.⁶ Some of the aforementioned oxides were found to be also effective in phosphorus removal, namely BaO,^{5,6,9} Al₂O₃,^{3,6} and MgO.^{5,6} The mechanism of slag refining for boron is well understood^{7,10} as can be seen from the studies of electronic-grade

silicon (EG-Si) doped with boron; the same mechanism is suggested for removal of phosphorus.

Slag refining of MG-Si containing a large number of impurities has scarcely been studied, as most of the published data were obtained for high-purity EG-Si doped with only the impurities of interest. Slag refining of MG-Si from boron and phosphorus is usually studied without attention being paid to other impurities in MG-Si, their influence on the refining efficiency, or the microstructure of MG-Si in general. The Elkem Solar process uses slag refining with the main purpose of removing boron from metallurgical-grade silicon by continuously adding slag forming fluxes.¹¹ However, a large number of impurities in MG-Si could result in concurrent processes. The necessity of controlling the aluminium to iron ratio was mentioned in the Elkem patent as well.¹¹ Addition of Fe₂O₃ to the slag mixture resulted in the formation of FeSi₂ and was found to be effective for removal of phosphorus.⁵ These facts illustrate the complexity of the slag refining processes of MG-Si. Moreover, the

segregation of impurities in MG-Si in contact with slag was not studied sufficiently.

The aim of the present work is to validate the applicability of the slag refining approach in combination with controlled cooling and acid leaching to industrial MG-Si by studying the microstructure of MG-Si with respect to the precise location of impurities.

EXPERIMENTAL PROCEDURES

Master slags of the CaO-Na₂O-SiO₂ system with different Na₂O contents were prepared using proportions of the components suggested for the efficient removal of boron.⁷ CaO and SiO₂ were used as received (Fluka), and Na₂O was obtained by thermal decomposition of sodium carbonate purchased from Fluka. All oxides were thoroughly mixed using a ball mill, and the master slag was formed at 1400°C in 0.5 h under air atmosphere using an Al-sint crucible (99.7% alumina); 1-h dwell at 1000°C was applied during the heating to decompose sodium carbonate. The obtained master slag had uniform structure. The true concentration of Na₂O in the master slag was determined by x-ray fluorescence (XRF) analysis using a Panalytical Axios Max WD-XRF spectrometer, with data evaluation done using SuperQ5.0i/Omnian software. Loss of 7 wt.% to 11 wt.% Na₂O was detected due to its volatility, so that initial 10 wt.%, 20 wt.%, and 30 wt.% Na₂O resulted in 3.3 wt.%, 9.0 wt.%, and 20.8 wt.% in the master slag, respectively. X-ray diffraction (XRD) analysis of the master slags was performed as well. A mixture of slag components without the master slag formation ("mixture slag" hereinafter) was also used for comparison. Synthesized master slag was crushed and intimately mixed with the crushed MG-Si (MG-Si chunks, 98.5%; Alfa) using a ball mill in a proportion suggested by Teixeira and Morita.⁷ However, in the cited article no information was provided on the conditions for slag preparation. In the present work the slag and silicon were equilibrated at 1470°C for 1 h under argon atmosphere using an Alsint crucible followed by a controlled cooling step at a rate of 5°C/min. The density of the slags of this system is close to that of silicon, so that sharp segregation could not be achieved and slag inclusions remained in the refined silicon.⁹ Application of different "pulling" techniques was suggested for achieving higher purity of silicon and for enhancing the separation of slag to the bottom and walls of the crucible. Directional solidification⁹ and Czochralski crystal pulling² have been successfully applied, and silicon ingots purified from slag inclusion were obtained. In the present work, controlled cooling was applied to enhance the separation of the slag from the refined silicon and to promote segregation of impurities, taking into account that retrograde dissolution of impurities back to silicon during the directional solidification was not detected.⁹

After the slag refining experiments, MG-Si usually has a spherical shape inside a slag shell. A cross-section of the silicon sphere was polished with a final polishing step using 1- μ m diamond paste. The samples were analyzed by optical microscopy in reflectance mode using a Leica DM/LP microscope. Grain boundaries and inclusions were studied by scanning electron microscope (SEM), and the chemical composition of the impurity phases was determined using energy-dispersive x-ray spectroscopy (EDX; JEOL JSM 6500F). An electron beam with energy of 15 keV and beam current of 95 nA was used. Electron probe microanalysis (EPMA) measurements were performed with a JEOL JXA 8900R microprobe device using an electron beam with energy of 15 keV and beam current of 500 nA, while employing wavelength-dispersive spectrometry (WDS). The chemical composition for each analysis of the samples was determined using the x-ray intensities of the constituent elements after background correction relative to the corresponding intensities of reference materials had been performed. Obtained intensity ratios were processed with the matrix correction program CITZAF.¹²

Both the source MG-Si sample and the MG-Si treated with the slag were crushed using a ball mill employing a tungsten carbide-coated grinding jar and balls. The powders with particle size below 0.1 mm were leached with a solution containing 20% of both HCl and HF acids. The source MG-Si, MG-Si treated with a slag, the leaching solutions, and MG-Si after the acid leaching were all prepared according to the procedure proposed by Takahashi¹³ and analyzed by the inductively coupled plasma optical emission spectroscopy (ICP-OES) technique using a Spectro Arcos EOP spectrometer.

RESULTS AND DISCUSSION

Microstructure of MG-Si

The studied MG-Si had as major impurities Fe (2000–3000 ppm), Al (600–700 ppm), Ca (400–500 ppm), Ti (100–200 ppm), and other metallic impurities in the concentration range less than 100 ppm. Boron and phosphorus were present in the ~65 ppm and ~85 ppm range, respectively. The detailed chemical composition of the impurities in the MG-Si is described in the authors' previous work.¹⁴ The microstructure of the source MG-Si showed many small inclusions with average area ~400 μ m² and concentration of $\sim 4.26 \times 10^{-6}$ inclusion/ μ m², distributed randomly throughout the silicon matrix (Fig. 1a). The composition of intermetallic phases in the source MG-Si is described elsewhere, whereas FeSi₂ was the major impurity phase.¹⁴ The proposed mechanism of slag refining of silicon considers only oxidation of boron or phosphorus by the slag and incorporation of their oxides in the slag network. Little information is available about the behavior of other impurities.

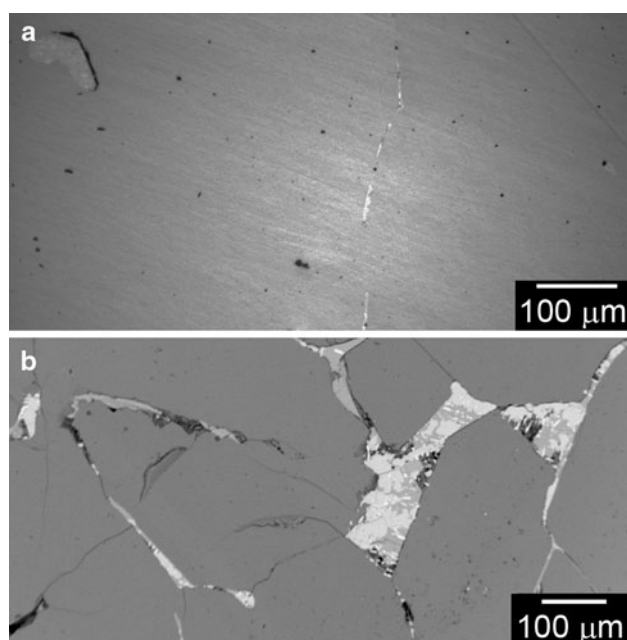


Fig. 1. Microstructure of MG-Si: (a) source, optical micrograph, (b) treated by 10 wt.% Na_2O mixture slag, SEM image.

Study of the microstructure of the material after the refining process is crucial for understanding the joint behavior of a large number of impurities in MG-Si during the treatment. Simple remelting of MG-Si with controlled cooling did not change the microstructure of MG-Si:¹⁴ impurities were still located in small randomly distributed inclusions, whereas boron and phosphorus were in the silicon matrix. The effect of the cooling rate on the behavior of impurities was studied in alloy refining of MG-Si with calcium.¹⁴ Comparison of the distribution of impurities is useful for understanding the mechanism of the processes taking place. In the present work, controlled cooling was applied at a rate of $5^\circ\text{C}/\text{min}$. Controlled cooling enables observation of the segregation processes of metallic impurities during the silicon treatment following the thermodynamic driving forces. Conventional slag refining is based on the liquid–liquid equilibrium between the slag and the metal, wherein the refined liquid metal is tapped and removed from the refining process.¹ However, a large number of impurities in MG-Si with low segregation coefficient in silicon (i.e., ratio between the concentration of an element in solid and liquid silicon)¹⁵ makes slag treatment with controlled cooling followed by acid leaching a promising and efficient refining method for all impurities. Controlled cooling allows growth of larger grains, which facilitates acid leaching. Large grains and pronounced grain boundaries do not require very fine grinding of silicon, which means less energy consumption and less silicon loss. Moreover, the controlled cooling enhances the separation of the slag from silicon,⁹ which is favorable for producing solar-grade silicon (SoG-Si) as well as

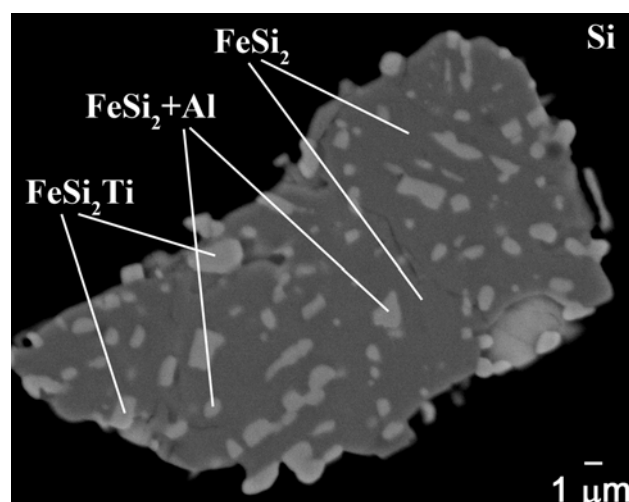


Fig. 2. Inclusion in the source MG-Si.

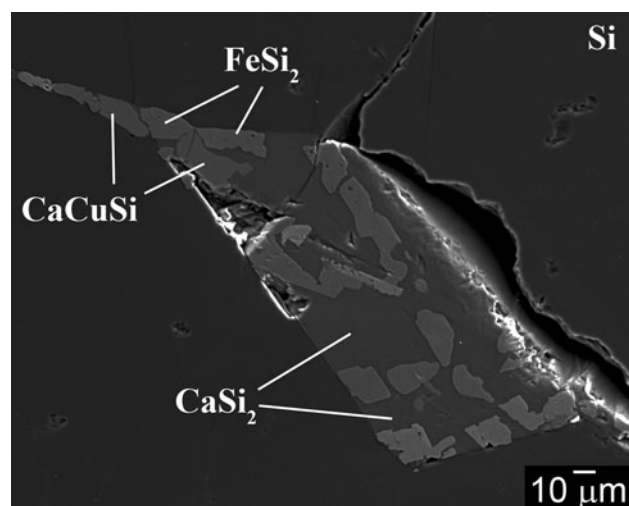


Fig. 3. Fragment of grain boundary in MG-Si treated with 3.3 wt.% Na_2O master slag.

for acid leaching. Finally, by combining the refining and segregation procedures in a one-step process, significant energy savings could be obtained due to minimization of the melting steps.

The microstructure of MG-Si after the treatment by the mixture slag containing 10 wt.% Na_2O is presented in Fig. 1b. The slag-treated MG-Si shows surprisingly large grain boundaries. The grain size after the treatment is approximately 1.5 mm^2 , which agrees with data on grain size using controlled cooling.¹⁴ Appearance of the clear grain boundaries indicates enhanced agglomeration of impurity phases and the formation of additional impurity phase during the slag treatment, since the total amount of impurity phases in MG-Si is insufficient to form clear grain boundaries (Fig. 1a). The structure of the grain boundaries and inclusions after the slag treatment is different compared with that in the source MG-Si (Figs. 2, 3). The impurity

phases precipitate in large clusters, segregated from each other and containing less scattered pieces of other phases than the inclusions in the source MG-Si (Fig. 2). This structure was observed for all slag-treated samples.

The slag preparation procedure influences the structure of grain boundaries in the resulting silicon: after the treatment with a mixture slag, the grain boundaries contain small pieces of impurity phases scattered inside the major ones in higher amount than in the case of the master slag (Fig. 3). The microstructure of the grain boundaries in the slag-treated MG-Si, in general, is still close to that of the source MG-Si (Fig. 2) with the exception that the CaSi_2 phase was found in the slag-treated MG-Si along with the known major impurity phase FeSi_2 .^{14,16} The chemical composition of the impurity phases in MG-Si treated with 10 wt.% Na_2O mixture slag is presented in Table I.

The content of CaSi_2 phase is comparable to that of FeSi_2 phase (Fig. 3), and several times higher than in the source MG-Si. Taking into account the volatility of calcium, CaSi_2 phase should be produced during the slag treatment. CaSi_2 phase was observed in grain boundaries of all the slag-treated MG-Si samples at all concentrations of Na_2O . Other impurity phases with high calcium content were also detected: Ca-Fe-Si-Ti, Ca-Cu-Si, Ca-Fe-Si, etc. (Table I). Impurity phase FeSi_2Ti observed in the source MG-Si was found again. No phase with high aluminum content was found, in contrast to the impurity phases in the source MG-Si,¹⁴ which could indicate removal of aluminum to the slag phase. Low sodium content was detected in three phases, usually together with high Ca content. Assuming that an additional amount of calcium was produced in the reaction with the slag, the co-appearance of calcium and sodium would be a logical observation.

Master slags with 3.3 wt.% (10 wt.% initially), 9.0 wt.% (20 wt.% initially), and 20.8 wt.% (30 wt.% initially) Na_2O were synthesized to obtain a slag network structure. The composition of the impurity phases in MG-Si treated with 3.3 wt.% Na_2O master slag showed many impurity phases with high calcium content [CaSi₂, Ca-Si (Si-rich), Ca-Fe-Ti-Si, Ca-Fe-Si, Ca-Cu-Si, Al-Ca-Si, Al-Fe-Ca-Si, Al-Ca-Fe-Si], which were not present in the source MG-Si. The increase of calcium content after the slag treatment was independent of the slag preparation method (master slag or mixture slag). CaSi_2 phase produced during the treatment could interact with impurity phases, resulting in the formation of a large number of Ca-rich intermetallic silicide phases. Various FeSi_2 -based phases with traces of Zr, Pt, and Al were detected in the grain boundaries of MG-Si treated with 3.3 wt.% Na_2O master slag; various mixed phases containing Ca, Fe, Ti, and Cu were observed as well. Dissolution of many transition metals in the iron-containing phases was also detected for the remelted MG-Si,¹⁴ in good agreement with the relatively low segregation coefficients

Table I. Composition (wt.%) of major impurity phases in MG-Si treated with 10 wt.% Na_2O mixture slag

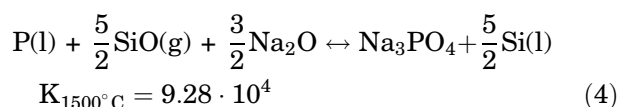
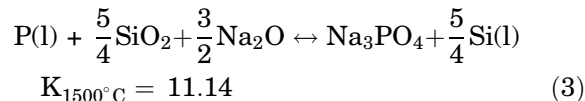
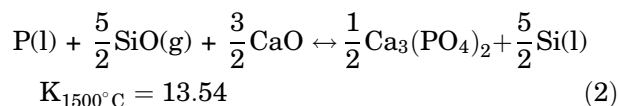
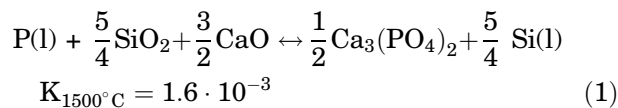
Element	O	Na	Al	Si	Ca	Ti	Fe	Other
FeSi_2			0.6 ± 0.4	49.3 ± 0.9	0.1 ± 0.1		48.3 ± 0.6	1.6 ± 0.3 (Mn), 0.1 ± 0.2 (Cr)
CaSi_2	0.5 ± 0.5	2.1 ± 0.2	0.1 ± 0.1	54.0 ± 0.7	42.1 ± 1.6	0.1 ± 0.2	1.1 ± 0.9	
FeSi_2Ti	0.1 ± 0.2			31.8 ± 1.0	0.6 ± 0.6	27.9 ± 1.6	34.0 ± 0.9	1.7 ± 0.2 (Mn), 2.1 ± 0.4 (V)
Ca-Fe-Si-Ti				35.9 ± 2.6	13.3 ± 6.0	20.6 ± 4.3	24.6 ± 4.9	1.4 ± 0.2 (Mn), 2.3 ± 0.7 (V)
Ca-Cu-Si	0.8 ± 0.5		1.5 ± 0.7	36.6 ± 0.9	40.4 ± 3.2		1.8 ± 0.8	3.3 ± 0.8 (Ni), 15.7 ± 1.5 (Cu)
Ca-Fe-Si		0.5 ± 0.3	0.7 ± 0.5	49.6 ± 1.3	10.3 ± 0.9		37.1 ± 1.2	1.7 ± 0.6 (Mn)
Ca-Fe-Na-Si-Ti-O	2.1 ± 0.5	3.6 ± 0.4		52.4 ± 2.2	21.1 ± 0.7	9.3 ± 0.5	10.3 ± 3.1	0.4 ± 0.2 (K), 0.8 ± 0.5 (V)

in silicon of most transition metals and the similarity in the crystal structure of their silicides.¹⁵ A Fe-Ti-Si-O phase containing 11.1 wt.% oxygen was found in grain boundaries, confirming the interaction of metallic impurities with slag.

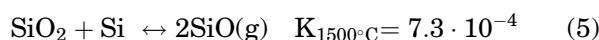
Chemical composition analysis of major impurity phases in grain boundaries of 9.0 wt.% Na₂O (20 wt.% initially) master slag-treated MG-Si showed a large number of intermetallic phases containing Fe, Ti, Al, Sb, and Sn. CaSi₂ phase was visually slightly less present than in grain boundaries of MG-Si treated with master slag containing 3.3 wt.% Na₂O (Fig. 3). Nevertheless, seven intermetallic phases with high calcium content were detected, whereas one phase (Ca-Cu-Si-O) had both high copper and oxygen concentration. This is an indication that the origin of the additional calcium is the slag. The iron-based phases contained traces of a series of transition elements, similar to the results of the study of impurity phases in MG-Si treated with master slag with 3.3 wt.% Na₂O.

The microstructure of MG-Si treated with 20.8 wt.% (30 wt.% initially) Na₂O master slag showed some typical inclusions and grain boundary structures (Fig. 3), as well as inclusions similar to those in the source MG-Si with lots of small pieces of one phase scattered within other phases (Fig. 2). The presence of such inclusions could be a result of insufficient time for segregation; however, at the same cooling rate for all experiments (5°C/min) it could be due to a decrease of the concentration of an agglomerating agent, i.e., light metal forming intermetallic phases. Calcium is one such metal, whose agglomerating influence on impurity phases was observed during Ca alloying of MG-Si.¹⁴ The chemical composition of the detected impurity phases in MG-Si treated with 20.8 wt.% Na₂O master slag shows FeSi₂ as the main phase, as in the case of lower initial Na₂O concentrations in the slag. The variety in the mixed Ca-Ti-Fe-Si phases differed compared with the results of alloying of MG-Si with calcium. During the Ca alloying study it was found that calcium and titanium behave as antagonists in silicide phases, whereas during slag treatment they were found in the same intermetallic phase. Such different behavior could be a result of different initial concentrations of calcium in silicon: 3 wt.% to 10 wt.% during Ca alloying and ~400 ppmw in the source MG-Si. The other phases detected were quite similar to the phases detected in MG-Si treated with slag with lower Na₂O content.

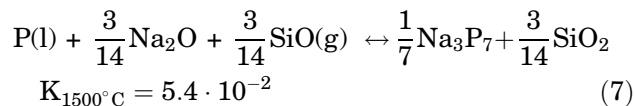
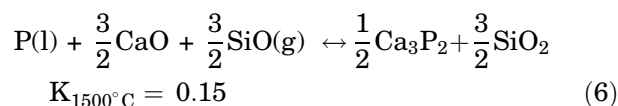
To explain the chemical processes during the slag treatment, possible chemical reactions and their constants were calculated using HSC Chemistry 6.1 software.¹⁷ Conventional slag refining of MG-Si is described as an oxidation process of boron and phosphorus dissolved in the silicon melt using the oxidation potential of the slag.^{6,7,18} Boron and phosphorus oxides are network formers¹ and incorporate into the slag structure. For phosphorus the same mechanism is proposed:¹⁷



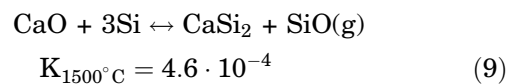
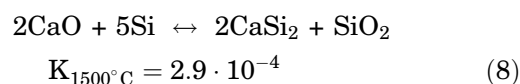
The equilibrium constants of reactions (2–4) are high, and thus these reactions will take place with high thermodynamic potential; however, reactions (2) and (4) are limited by a concentration of silicon monoxide.

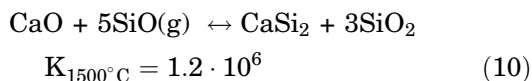


Several stable compounds of phosphorus with the slag-forming elements are known, and their reactions of formation are also limited by the amount of silicon monoxide:



Moreover, a number of parallel reactions are possible, taking into account the value of their reaction constants:





Reactions resulting in CaSi_2 formation explain where the additional grain boundary material originated. It was observed that alloying of MG-Si with a small addition of calcium already resulted in agglomeration of inclusions and enhanced segregation of impurity phases in inclusions and grain boundaries.¹⁴ Pronounced grain boundaries were observed with calcium addition of ~ 5 wt.%. The values of the constant of reactions (8) and (9) agree well with the observation of the formation of a few weight percent of CaSi_2 during the slag treatment. Reaction (10) has a high constant, but is limited by the amount of silicon monoxide produced by reaction (5). Both oxidation of phosphorus (reactions 2 and 4) and CaSi_2 formation (reaction 10) depend on the SiO concentration; hence, these processes compete with each other.

Another important argument speaks in favor of the proposed mechanism: in all impurity phases detected after the slag treatment, the highest sodium content is in the Ca-rich phases. CaSi_2 phase shows the highest contents: 2.1 wt.% when using 10 wt.% Na_2O mixture slag and 1.5 wt.%, 0.9 wt.%, and 1.5 wt.% when using 3.3 wt.%, 9.0 wt.%, and 20.8 wt.% Na_2O master slag, respectively. This is a solid confirmation that reactions (8–10) take place. Other Ca-rich phases also contain relatively high amounts of dissolved sodium: Ca-Fe-Na-Si-Ti-O (3.6 wt.%), Ca-Si (Si-rich) (0.8 wt.%), Ca-Fe-Ti-Si (1.1 wt.%), Ca-Fe-Si (0.17 wt.%), etc. The high sodium content of Ca-rich phases can only occur when the CaSi_2 phase is formed in interaction with liquid slag, where sodium is evenly distributed. Other phases Sb-Si-O, Cu-Sb-Si-O, Ca-Cu-Si-O, and Fe-Ti-Si-O with relatively high sodium content (0.4–0.9 wt.%) have high oxygen contents, together with or without copper or antimony. The high oxygen content again points to the origin of the sodium being the slag structure.

In conclusion, after treatment with slag of the Na_2O -CaO-SiO₂ system, significant changes occur in the microstructure of MG-Si. Enhanced segregation of impurities and formation of CaSi_2 and various Ca-containing impurity silicide phases were observed.

Detection of Boron and Phosphorus

Some impurity phases in the grain boundaries of MG-Si treated with slag showed the presence of 0.1 wt.% to 2.0 wt.% phosphorus. These phases often contained both iron and titanium or calcium-aluminum silicides. Similar behavior was observed in MG-Si alloyed with calcium.¹⁴ Similar observations were discussed in the authors' previous work¹⁴ using Ca-alloying of MG-Si, being attributed to a chemical affinity of phosphorus to dissolve in these

phases. The highest phosphorus concentration of 2 wt.% was detected in the Al-Ca-Si phase. The observation of phosphorus in a nonoxidized state in grain boundaries after the slag treatment points to a concurrent capture process for phosphorus. In the case of phosphorus oxidation by a slag, controlled cooling could not lead to its retrograde reduction, and the oxidized phosphorus will remain in a phosphate structure. Additionally, two grain boundary phases containing oxygen showed chemical affinity to phosphorus: Fe-Si-Ti-O and Sb-Si-O. The nature of their affinity to phosphorus is not yet clear; however, the Fe-Si-Ti-O phase could be a modification of the FeSi_2Ti phase, which was able to dissolve up to 0.4 wt.% phosphorus.¹⁴ Antimony does not form any binary compounds with phosphorus,¹⁹ and hence the synergy of phosphorus dissolution should lie in its oxide. No phosphorus was found in the CaSi_2 phase, previously determined to be a getter phase for phosphorus.²⁰ In the presence of the large number of impurities in MG-Si, CaSi_2 phase plays only an intermediary role in the transport of phosphorus.¹⁴ No correlation of the phosphorus content with the concentration of Na_2O was found.

EPMA study of the impurity phases in the source MG-Si²¹ showed that impurity phases based on FeSi_2 and FeSi_2Ti contained up to 1.0 wt.% to 2.5 wt.% boron. The boron content in the FeSi_2 phase increased up to 2.7 wt.% after the slag treatment.²¹ The detection of boron and phosphorus in impurity phases indicates their concurrent interactions with intermetallic silicide phases. These intermetallic compounds could be effective in refining of MG-Si with any composition of impurities from boron and phosphorus.

Microstructure of Slag after the Slag Treatment

The microstructure of the resulting slag was analyzed by SEM-EDX to determine the main phases and distribution of the slag components. Taking into account the ratio of slag to MG-Si of 2.3 and the very low total concentration of both boron and phosphorus, it was difficult to detect boron and phosphorus in the slag. Mixture slag with 10 wt.% Na_2O had a dendrite-like microstructure, showing two main phases: dendrite phase (Fig. 4, "light" phase) and a cellular phase present between the dendrites (Fig. 4, "dark" phase, inset). The dendrites consisted of calcium silicate and did not contain any sodium, which in turn had a maximum concentration of 9.9 ± 1.3 wt.% in the second abundant Al-Ca-Na-Si-O phase. This "dark" Na-rich phase contained 12.9 ± 2.2 wt.% aluminum, which could indicate efficient aluminum removal from MG-Si. Detected minor phases Al-Ca-Si-O, Ca-Na-Si-O, and Al-Ca-Na-Si-O differ from the calcium silicate phase in the amount of sodium and aluminum.

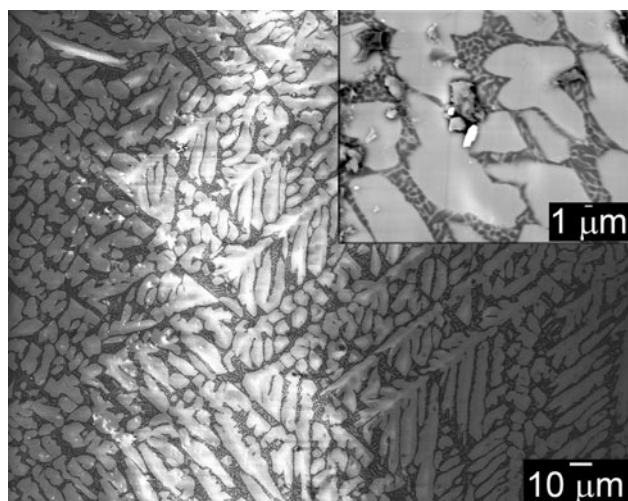


Fig. 4. Mixture slag with 10 wt.% Na_2O after the slag treatment; inset increased magnification.

Master slag with 3.3 wt.% Na_2O (10 wt.% Na_2O initially) after the slag treatment had a glassy and highly reflective structure (Fig. 5), common for silica-based slags.¹ The symmetry of the microstructure appeared quite similar to that of the mixture slag with the same initial Na_2O content (Fig. 4). To make the slag less viscous and enhance the slag-silicon interaction, addition of fluxes^{3–5,7} has been suggested, as they break the slag network. Alkaline oxides are also known as network breakers; however, an initial concentration of 10 wt.% Na_2O resulted in 3.3 wt.% Na_2O and high viscosity of the slag: silicon spheres were observed stuck in the slag (Fig. 5, inset). Using controlled cooling, silicon solidifies as a first component and silicon nuclei agglomerate in spheres, even though the viscous slag structure limits their agglomeration. The major phase after the slag treatment of MG-Si was calcium silicate, and its three modifications with various concentration of aluminum were detected in minor amounts.

Higher Na_2O content provides lower viscosity to the master slag, which facilitates slag-silicon separation during cooling. No entrapped silicon spheres were found in master slags with >3.3 wt.% Na_2O . The microstructure of the master slag changed with the concentration of sodium oxide: a fine hexagonal-like microstructure at 3.3 wt.% transformed into a block-like fragmented structure at 9.0 wt.%, ending as a soft dendrite-like structure at 20.8 wt.%. Master slags with high Na_2O content consisted of two phases: Na-containing “dark” and “light” calcium silicate phase (SEM images) and “dark” phase containing 12 wt.% to 13 wt.% aluminum.

Master slags with 9.0 wt.% and 20.8 wt.% Na_2O showed some traces of phosphorus on SEM-EDX after the refining treatment. This confirms the oxidation of phosphorus by the slag (reactions 1–4). At the same time, the detection of higher phosphorus amounts in the intermetallic phases indicated

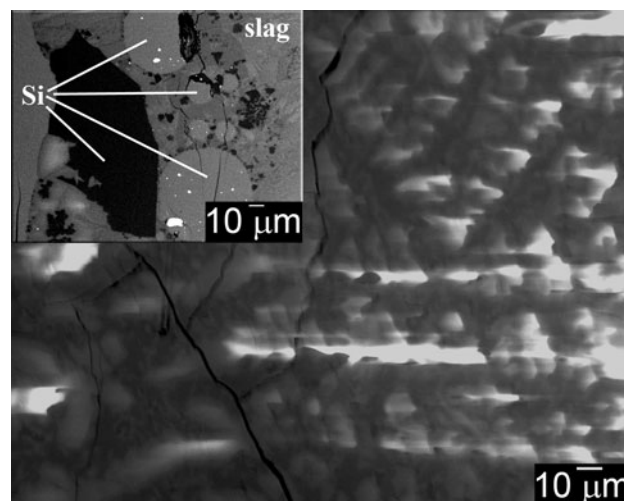


Fig. 5. Master slag with 3.3 wt.% Na_2O after the slag treatment; inset silicon spheres entrapped in the slag.

the competitive process. The silicon matrix after the slag treatment was pure, with only some traces of oxygen being detected.

Acid Leaching

Acid leaching is known as a cheap method of refining of impure silicon, being based on the dissolution of soluble intermetallic phases, but it is not applicable to impurities dissolved in the silicon matrix.²² The efficiency of acid leaching is higher if silicon is alloyed with a small amount of calcium addition.²⁰ The added metal forms silicide-based grain boundaries, where impurities from MG-Si precipitate. In the present work, acid leaching was applied to the samples of MG-Si treated with slag of the Na_2O -CaO- SiO_2 system. Analysis of the combination of slag treatment with acid leaching as a refining route of MG-Si is performed for the first time, together with analysis of the MG-Si microstructure.

The MG-Si samples before the treatment, after the slag treatment, and after the acid leaching, as well as the leach-out solutions, were analyzed for their content of impurities using ICP-OES. The initial concentration of impurities in the source MG-Si is published elsewhere,¹⁴ where iron was the major impurity. After slag treatment, the concentrations of Al, Ca, Na, and Mg increased significantly (Fig. 6). Although the Na_2O concentration in master slag is lower than in mixture slag, the increase of Al, Ca, Na, and Mg is greater for the master slag. The acid leaching process removed the major part of the impurities in grain boundaries, and the resulting silicon usually showed the lowest concentrations of all impurities with the exception of Al, Ca, and Na.

After slag treatment, the concentration of calcium exceeded by 10–30 times its content in the source MG-Si (542 ppmw) and reached a maximum of

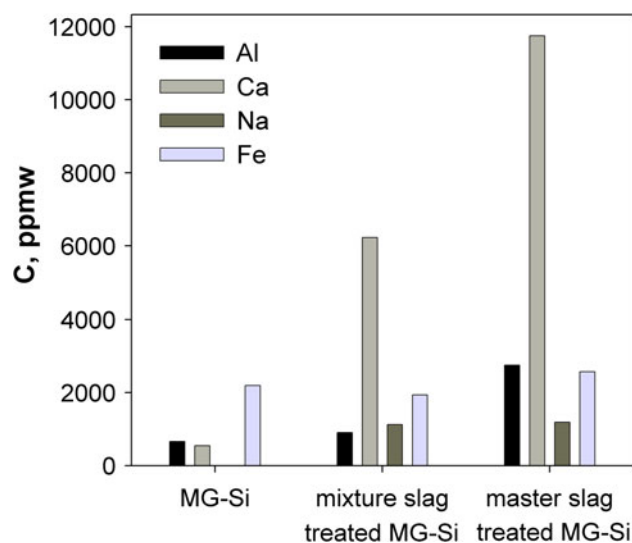


Fig. 6. Major impurities in MG-Si treated by mixture and master slag with 10 wt.% Na_2O initially.

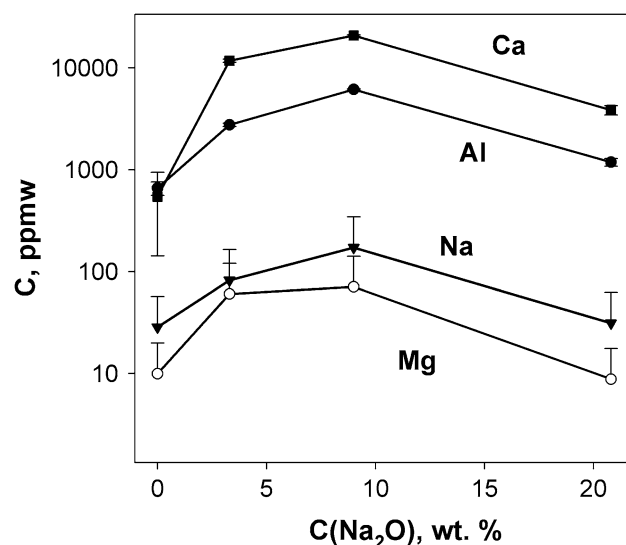


Fig. 7. Concentrations of Al, Ca, Mg, and Na in MG-Si treated by a master slag with different Na_2O contents.

~2 wt.% when using the master slag with 9.0 wt.% Na_2O (20 wt.% initially) (Fig. 7). The concentration of aluminum increased by several times in comparison with its level before the treatment (658 ppmw) and again reached its maximum after the treatment with the master slag with 9.0 wt.% Na_2O (6131 ppmw). The concentrations of Fe, Ti, Cu, V, and Zr found in the source MG-Si did not change much after the slag treatment; their variation presents the unevenness of the distribution of impurities in the MG-Si. Sodium was present in the source MG-Si at 1 to 2 ppmw, but after the slag treatment its content reached a maximum of 2073 ppmw when using the 9.0 wt.% Na_2O master slag. The contents of Ca, Na, and Al in the total sample after slag treatment consisted cumulatively of the amounts present in grain boundaries along with those dissolved in the silicon matrix. The sum of the analyses of the leach-out solutions and the leached silicon confirmed this statement as well as the removal of the major part of all impurities by acid leaching. The level of impurities after the acid leaching represented the concentration of impurities dissolved in the silicon matrix. The influence of the Na_2O content in the slag on its content in the silicon could be explained by differences in the slag structure: at small amounts of Na_2O , it dissolves in calcium silicate-based phases, and at 20.8 wt.% it forms a NaCaSiO_4 phase, which should have stronger connection with sodium. This phase was observed in the XRD pattern of this master slag.

The increase of the calcium concentration was in accordance with the proposed chemical reactions resulting in formation of CaSi_2 phase (reactions 7–9). Sodium, apparently, diffuses from the slag structure into the grain boundaries and dissolves, up to a limited content, in the silicon matrix. The solubility of sodium in silicon is 152 ppmw at

1200°C,²³ so slightly below the melting point of silicon it could be up to 200 ppmw. Aluminum might come from the crucible material; however, during the master slag preparation no interaction of the slag component with the crucible was observed. During the treatment of MG-Si with the master slag, the liquid state of the slag enhanced the interaction with alumina and facilitated its diffusion into silicon, resulting in extended dissolution of aluminum in silicon. Despite this fact, the detected concentration of sodium in the mixture slag-treated MG-Si was almost the same as when using the master slag (Fig. 6). Although the concentration of Na_2O in the master slag was lower than in the mixture slag with the same initial Na_2O content, the lower melting point of the master slag and hence longer contact time with silicon resulted in almost the same level of sodium in the silicon after both of these treatments. The high concentration of calcium confirmed the observed formation of CaSi_2 and other Ca-rich phases. The increased amount of sodium after the slag treatment could be assigned to its enhanced diffusion from the liquid master slag. The level of other metallic impurities originally present in MG-Si was not affected by the slag treatment because of their higher Gibbs energy of oxide formation compared with the slag components (Ellingham diagram²⁴). For titanium, the Gibbs energy for the formation of its oxide is slightly below that of silicon, so that minor titanium oxidation correlates with the detection of the Fe-Si-Ti-O phase in MG-Si after the slag treatment.

For boron and phosphorus, the refining process is illustrated in Fig. 8 for both mixture slag and master slag treatments with 10 wt.% Na_2O initially. It is evident that the concentrations of both boron and phosphorus were higher when using the master slag, which could be due to the lower Na_2O content:

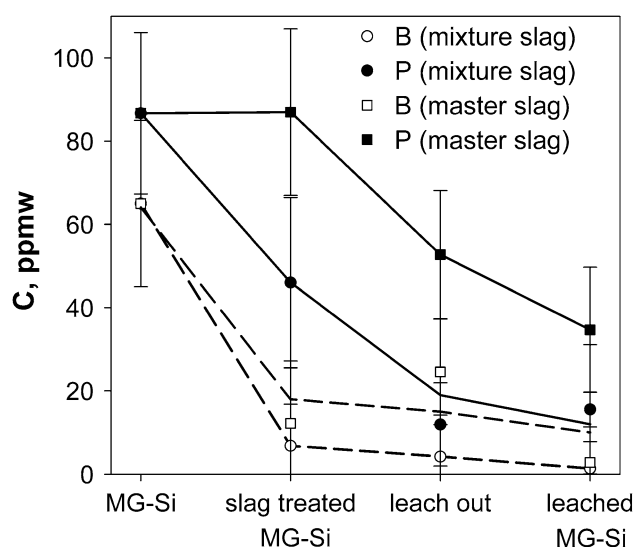


Fig. 8. Concentrations of B and P in source MG-Si, MG-Si treated with mixture, and master slag with 10% Na_2O initially, leach-out solutions, and leached MG-Si.

10 wt.% resulted in 3.3 wt.% Na_2O after the master slag formation. The slag viscosity could also play a role: the master slag was viscous, and the silicon spheres stuck in the slag (Fig. 5, inset), whereas the mixture slag provided good mixing of the components by decomposition of sodium carbonate resulting in CO_2 gas formation.

The kinetics of the refining process for boron and phosphorus was different. The boron content was greatly reduced (more than 70–80%) after both slag treatments, after which little further decrease is detected on applying the acid leaching treatment. According to the results on the partition ratio for boron using Na_2O -CaO- SiO_2 slags,⁷ the predicted concentration of boron in the final silicon is about 20 ppmw. In the present work the lowest values obtained were: 6.8 ± 10 ppmw for the 10 wt.% mixture slag and 12 ± 10 ppmw for the 3.3 wt.% master slag. The additional boron removal could be assigned to its dissolution in intermetallic compounds.²¹ At the same time, the changes in the phosphorus concentration after the slag treatment did not exceed 50% when using a mixture slag, and were almost zero when using the master slag. Almost half of the total phosphorus content was removed after the acid leaching treatment. The sum of the concentrations in the leach-out solution and leached silicon confirms the accuracy of the experiments (Fig. 8). The different refining behavior of boron and phosphorus confirms the efficiency of the slag refining process for boron, but indicates a different mechanism of refining for phosphorus.

After the leaching treatment, the concentration of all impurities in MG-Si treated by master slag decreased, but the concentrations of Al, Ca, and Na were still higher than in the source MG-Si (Fig. 9). With increase of the Na_2O concentration in the master slag up to 9.0 wt.%, the concentrations of Al,

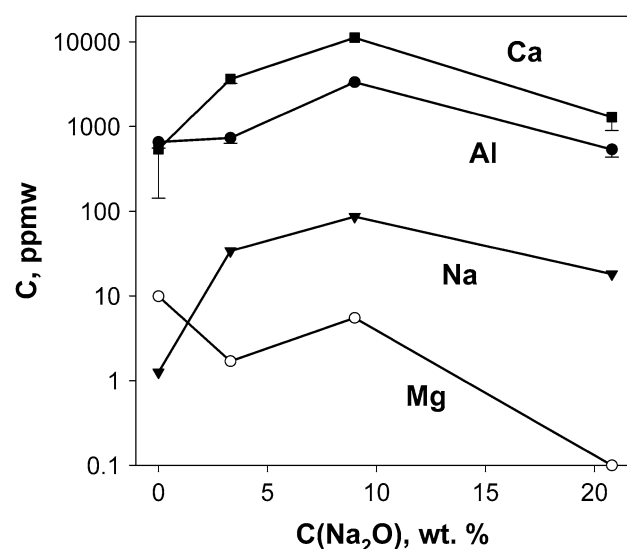


Fig. 9. Concentrations of Al, Ca, Mg, and Na in MG-Si treated by a master slag with different Na_2O contents and leached.

Ca, and Na remaining in the silicon also increased and were proportional to the total produced concentration of these elements (Fig. 7). This fact can be attributed to the lower melting point of the master slag with 9.0 wt.% Na_2O resulting in a longer contact time with silicon. The master slag with 20.8 wt.% Na_2O gave the lowest values for sodium and calcium, which were, however, still above their level in MG-Si. This improvement of concentration correlates with the different master slag structure compared with that of the master slags with lower Na_2O content as detected by XRD pattern analysis. When using the treatment with the master slag with 20.8 wt.% Na_2O followed by leaching, the concentration of aluminum was reduced to a level below its concentration in the source MG-Si. Magnesium was efficiently removed by acid leaching; at 20.8 wt.% Na_2O , its concentration was below 1 ppmw.

The concentrations of Cu, Fe, Ti, V, and Zr were also efficiently reduced when using slag treatment with controlled cooling followed by acid leaching. The lowest content of these elements was achieved at 3.3 wt.% and 20.8 wt.% concentration of Na_2O in master slag. These elements segregate well, and the obtained results agree well, with the exception of the master slag containing 9.0 wt.% Na_2O .

The behavior of boron and phosphorus at different concentrations of sodium oxide in the master slag is shown in Fig. 10. Phosphorus can be efficiently refined using the suggested approach, and its concentration decreased almost exponentially with increasing Na_2O concentration. The presented efficient removal of phosphorus is in good agreement with the detection of a high amount of phosphorus in Al-Ca-Si and FeSi_2Ti grain boundary phases. This effect could be assigned to the formation of CaSi_2 phase facilitating the phosphorus transfer.¹⁴

The positive influence of calcium addition on phosphorus removal was described elsewhere.^{11,25,26} In the present work a combination of slag refining and alloying refining is realized in a one-step process, and together with controlled cooling and acid leaching provides a basis for a new route for upgrading MG-Si to solar-grade silicon. Results were not as straightforward for boron: its concentration was lower after the overall treatment; however, at 9.9 wt.% and 20.8 wt.% Na₂O it was higher than for 3.3 wt.%.

A comparison of the results using the different slag preparations is presented in Table II. Average concentrations (*c*) of the most harmful impurities in the refined silicon after the process sequence of slag treatment, controlled cooling, and acid leaching are presented along with the refining efficiency (η). Not detected (n.d.) values in the table refer to concentrations below the detection limit, which is 1 ppmw for the ICP-OES technique for most of the presented

elements. The efficiency of the refining process (η) was calculated as the percentage ratio of the element concentration in the refined silicon to that in the source MG-Si. For the impurities Al, Ca, Na, and Mg, whose concentrations significantly increased during the slag treatment, the refining efficiency η was calculated based on the level of impurities in the slag-treated MG-Si.

The presented results show quite good refining efficiency for all the experimental conditions. Most of the metallic impurities were removed from MG-Si completely, independently of the slag composition, because the controlled cooling enhanced their segregation. Titanium removal is at its lowest (95%) for the mixture slag with 10 wt.% Na₂O and reaches 100% when using a master slag with high (9.9 wt.% and 20.8 wt.%) Na₂O concentration. The Gibbs energy of oxide formation for titanium is slightly below that for silicon, so that titanium could be partly oxidized by a slag in addition to its segregation to grain boundaries; this combination of processes could better explain the refining efficiency found when using a master slag. The longer contact time with silicon when using the master slag is favorable for titanium removal as well, taking into account the low diffusivity of titanium in silicon.¹⁵ Since the concentrations of Al, Ca, Na, and Mg in MG-Si increased during the slag treatment, they are more difficult to refine. In this sense, the mixture slag with 10 wt.% Na₂O gave the best results, and the final concentrations of sodium and aluminum were below their solubility in silicon.^{15,23}

The mechanism of refining is different for boron and phosphorus: phosphorus removal increased significantly with increasing concentration of Na₂O in the master slag, whereas boron removal was better when using mixture slag with 10 wt.% Na₂O. The total concentration of aluminum and calcium significantly increased after the slag treatment, and could be minimized when using the mixture slag. Most likely, this is connected with the contact time with silicon. Magnesium and sodium also entered MG-Si during the slag treatment; nevertheless, they can be removed efficiently during acid leach-

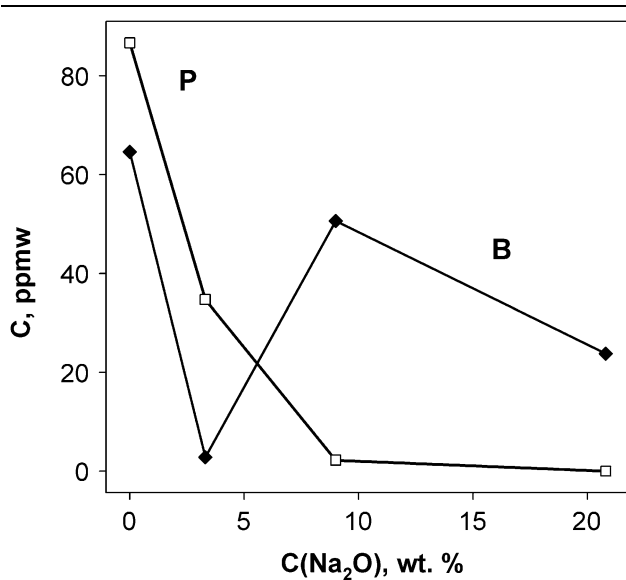


Fig. 10. Concentrations of B and P in MG-Si treated by a master slag with different Na₂O contents and leached.

Table II. Impurities composition of the refined MG-Si (*c*, ppmw) and refining efficiency of the slag treatments followed by acid leaching (η , wt.%)

Slag Type		Impurity								
		Al	B	Ca	Fe	Mg	Na	P	Ti	Co, Cr, Ni, Mo, Mn
Mixture slag, 10 wt.% Na ₂ O	<i>c</i>	46	1	132	n.d.	n.d.	9	16	10	n.d.
	η	94.9	97.9	97.9	100	99.6	99.2	82.1	95	100
Master slag, 3.3 wt.% Na ₂ O	<i>c</i>	734	3	3634	n.d.	2	34	35	2	n.d.
	η	73.3	95.7	69.1	100	97.2	97.1	60	99.1	100
Master slag, 9.9 wt.% Na ₂ O	<i>c</i>	3340	51	11195	3	5.5	86	2	n.d.	n.d.
	η	45.5	21.5	46.0	99.9	92.2	95.8	97.4	100	100
Master slag, 20.8 wt.% Na ₂ O	<i>c</i>	536	24	1293	n.d.	n.d.	18	n.d.	n.d.	n.d.
	η	54.7	63.1	66.3	100	100	97.8	100	100	100

ing. No dependence of the removal efficiency on the concentration of sodium oxide in the slag was found: even though their concentration after the slag treatment increased, more than 92% of magnesium and sodium could be removed using acid leaching. The difference in the behavior of calcium and aluminum on one hand and sodium and magnesium on the other hand could be a result of their preferred dissolution: sodium and magnesium apparently dissolve better in impurity phases, whereas calcium and aluminum at their high concentrations dissolve in the silicon matrix.

CONCLUSIONS

In the present work, the mechanism of slag treatment of MG-Si was investigated using analysis of the microstructure of MG-Si. Formation of CaSi_2 and Ca-rich phases during the slag treatment was observed. This fact should be taken into account when modeling slag-silicon interactions. It is indicated that a refining approach consisting of slag treatment with controlled cooling followed by an acid leaching procedure has great potential to refine MG-Si to SoG-Si. The mechanism of removal of impurities is determined based on the realized combination of slag oxidation treatment, alloying with calcium, and segregation processes. The experimental results indicate the possibility of reaching concentrations for most impurities in the ranges required for SoG-Si. The suggested approach can efficiently refine boron, phosphorus, and most metallic impurities from MG-Si across a broad range of concentrations. However, control of the Al, Ca, and Na concentrations is required. An alternative mechanism for refining for phosphorus is suggested based on its affinity to dissolve in intermetallic Al-Ca-Si and FeSi_2Ti phases. However, various factors influence the efficiency of the refining process: the Na_2O concentration, the mixing intensity of the molten slag and silicon, slag properties (melting temperature, basicity, viscosity, and interfacial tension), and the treatment time, all of which require careful control and optimization.

ACKNOWLEDGEMENTS

This research was carried out under project number M71.5.08316 in the framework of the Research Program of the Materials innovation institute (M2i, www.m2i.nl). The authors would like to thank the following staff at the Delft University of Technology: Ir. C. Kwakernaak for help with EPMA measurements, Ir. J. Padmos and M.M. van

den Brink for ICP-OES analyses, Ir. R.W.A. Hendrikx for XRF and XRD measurements, and Dr. G. Zimbitas as a native speaker for correction of article language.

OPEN ACCESS

This article is distributed under the terms of the Creative Commons Attribution License which permits any use, distribution, and reproduction in any medium, provided the original author(s) and the source are credited.

REFERENCES

1. T.A. Engh, C.J. Simensen, and O. Wijk, *Principles of Metal Refining* (Oxford University Press, 1992), Chap. 2.
2. H.M. Liaw and F. Secco D'Aragona, *Solar Cells* 10, 109 (1983).
3. R. Noguchi, K. Suzuki, F. Tsukihashi, and N. Sano, *Metall. Mater. Trans. B* 25B, 903 (1994).
4. A. Schei, US patent 5788945, Aug. 4, (1998).
5. E. Enebak, US patent application 2008/0156145 (2008).
6. M.D. Johnston and M. Barati, *Sol. Energy Mater. Sol. Cells* 94, 2085 (2010).
7. L.A.V. Teixeira and K. Morita, *ISIJ Int.* 49, 783 (2009).
8. Y. Hu, D. Lu, T. Lin, Y. Liu, B. Wang, C. Guo, Y. Sun, H. Chen, and Q. Li, *Adv. Mater. Res. (Durnten-Zurich, Switz.)*, 156–157, 882 (2011).
9. R.K. Galgali, B.C. Mohanty, J.L. Gumaste, U. Syamaprasad, B.B. Nayak, S.K. Singh, and P.K. Jena, *Sol. Energy Mater.* 16, 297 (1987).
10. L.A.V. Teixeira, Y. Tokuda, T. Yoko, and K. Morita, *ISIJ Int.* 49, 777 (2009).
11. J. Smith, S. Johnson, and S. Oxman, US patent 5820842. (1998).
12. J.T. Armstrong, *Electron Probe Quantitation*, ed. K.F.J. Heinrich and D.E. Newbury (New York: Plenum, 1991), p. 261.
13. J. Takahashi, *Agilent ICP-MS Journal* (Agilent Technologies Inc., 2008), p. 2.
14. Y.V. Meteleva-Fischer, Y. Yang, R. Boom, B. Kraaijveld, and H. Kuntzel, *Intermetallics* 25, 9 (2012).
15. W. Zulehner and D. Huber, *Crystals Growth, Properties and Applications*, Vol. 8, ed. J. Grabmaier (Berlin Heidelberg New York: Springer-Verlag, 1982), p. 1.
16. J.C. Anglezio, C. Servant, and F. Dubrous, *J. Mater. Res.* 9, 1894 (1990).
17. HCS Chemistry® 6.1, <http://www.hsc-chemistry.net/>.
18. T. Weiss and K. Schwerdtfeger, *Metall. Mater. Trans. B* 25B, 497 (1994).
19. B. Predel, *SpringerMaterials—The Landolt-Börnstein Database*, ed. O. Madelung. doi:10.1007/10542753_2377.
20. T. Shimpo, T. Yoshikawa, and K. Morita, *Metall. Mater. Trans. B* 2, 277 (2004).
21. Y.V. Meteleva-Fischer, Y. Yang, R. Boom, B. Kraaijveld, and H. Kuntzel, *EPD Congress 2012*, ed. L. Zhang, J.A. Pomykala, and A. Ciftja (Warrendale, PA: TMS, 2012), pp. 463–470.
22. J.M. Juneja and T.K. Mukherjee, *Hydrometallurgy* 16, 69 (1986).
23. J. Songster and A.D. Pelton, *J. Phase Equilib.* 13, 67 (1992).
24. H.J.T. Ellingham, *J. Soc. Chem. Ind.* 63, 125 (1944).
25. B. Ceccaroli and K. Friestad. US patent 6861040.
26. K. Zeaiter, US patent application 20110250118.